A NOVEL DECOMPOSITION SCHEME FOR IMAGE DE-NOISING

Radu Ciprian Bilcu, Markku Vehvilainen

Multimedia Technologies Laboratory
Nokia Research Center
Visiokatu 1, 33720, Tampere, Finland

ABSTRACT

In this paper we introduce a novel decomposition scheme for image de-noising. The processed image is decomposed in several components following a tree structure similar to wavelet decomposition. The main difference rely on the fact that image components are obtained at the output of some adaptive filters while wavelet decomposition uses filters with fixed frequency response. Moreover, in our approach the resolution of the different components is the same. The components are filtered separately and recombined to obtain the output image. The proposed de-noising scheme shows improved performances and simpler implementation compared to other approaches based on wavelet, contourlet and other image transforms.

***Index Terms*—** Image processing, image de-noising, image decomposition, directional filtering

1. INTRODUCTION

Due to the widespread of imaging devices (such as digital cameras, camera phones, etc) digital imaging has known an increased interest during the last decade. Although the manufacturing technology of the electronic components has been improved, the captured images still suffer from several distortions. Among many distortions, noise is one of the most important and can be introduced by several sources such as: the recording medium (film, digital sensor), transmission medium, measurement and quantization errors. Latest digital imaging sensors possess increased resolution (number of pixels per image) which is obtained by decreasing the pixel area. The cost of this is the increase of the sensor noise especially in low light conditions where the signal-to-noise ratio, at the output of a digital imaging sensor, can be extremely low. As a consequence, image de-noising is still an actual research topic in image processing community.

There are many publications dealing with the problem of noise reduction in images. In general, the existing algorithms and methods can be classified into two main categories: the approaches that operate on the input image directly [1, 2, 3, 4] and the methods that first transform the image and modify the components (see for instance [5, 6, 7, 8, 9, 10]).

A well known approach, that became reference in the field, is the de-noising based on wavelet shrinkage [5], [6]. In that approach the input image is decomposed into several components using wavelet decomposition. The wavelet coefficients are then modified to reduce the noise, and the output image is obtained by the inverse wavelet transform (IWT). Another approach that uses image decomposition was proposed in [8] where a bank of directional filters is used for image decomposition. Curvlet and contourlet transforms were also used for de-noising in [9] and [10] respectively. In a recent paper we have introduced a simple image decomposition scheme for image de-noising [7]. In the referenced paper, the main idea is to perform first a rough separation between the noise and the image content into different components. The components are then filtered separately according to their estimated noise level and detail content. The output image is then obtained by simply adding the filtered components.

In this paper we propose a novel decomposition scheme for image de-noising that shows good filtering results with low computational cost.

2. PROPOSED APPROACH

During the paper we assume that the input image is corrupted by an additive zero mean Gaussian distributed noise. The input image can be described by the following model:

$$y(i,j) = x(i,j) + n(i,j). \tag{1}$$

where $x(i,j)$, $y(i,j)$ and $n(i,j)$ are the original clean image, the observed image and the additive noise respectively.

2.1. Image decomposition

The de-noising method proposed in this paper uses a simplified decomposition scheme depicted in Fig. 1. The input image $y(i,j)$ is decomposed into three components $y_1(i,j)$, $y_2(i,j)$ and $y_3(i,j)$ which have the same resolution and are obtained in the following manner:

$$\begin{aligned} y_1(i,j) &= F\left(y(i,j)\right), \quad y_2(i,j) = F\left(y'(i,j)\right), \\ y_3(i,j) &= y'(i,j) - F\left(y'(i,j)\right). \end{aligned} \tag{2}$$

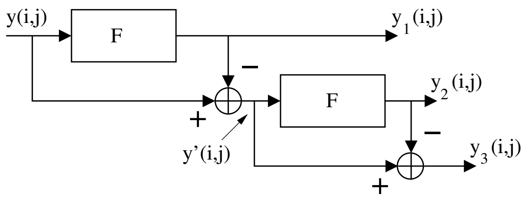

Fig. 1. The image decomposition block diagram.

where $y'(i,j) = y(i,j) - F(y(i,j))$ and $F(\bullet)$ is a 2D directional filter applied to the image inside the parentheses.

We note that, unlike the usual approaches that uses banks of different filters [8], in our method the same filter is implemented to obtain all image components. Briefly, the output of the selective filter $F(\bullet)$ is computed as follows: a rectangular $N \times N$ window is centered around the current pixel and four sub-windows are considered (the horizontal line, the vertical line and the two diagonals). The averages and variances of the four sub-windows are computed. The output at the current position is the average computed on the sub-window that have the smaller variance. We make here the following observation that is used further in the paper:

Obs: The output of the filter $F(\bullet)$, at certain pixel position, is the average of exactly N pixels and one of them is the current pixel.

Once $y_1(i,j)$, $y_2(i,j)$ and $y_3(i,j)$ are computed, similar or different processing techniques are applied to them in order to reduce the noise. It is clear from (2) and the above observation that $y_1(i,j)$ contains most of the image content (some of small features are eliminated and some edges are blurred) and a small level of noise. The component $y_2(i,j)$ contains a small level of noise and some of the missing features from $y_1(i,j)$. The last component $y_3(i,j)$ contains the rest of the image features and most of the noise. The variance σ_{n1}^2 of the noise in $y_1(i,j)$ is given by:

$$\sigma_{n1}^2 = \frac{1}{N}\sigma_n^2. \tag{3}$$

where σ_n^2 is the variance of the input noise component. The result from (3) comes directly from the above observation.

The variance of the noise in $y'(i,j)$ can be computed by:

$$\sigma_{n'}^2 = E\left\{(n'(i,j) - m_{n'})^2\right\}, \tag{4}$$

where $n'(i,j)$ and $m_{n'}(i,j)$ are the noise samples and their mean.

Let's assume that at current position the horizontal line was chosen by both filters from Fig. 1 (the other cases are identical to this). In this case the noise $n'(i,j)$ in $y'(i,j)$ can be written as:

$$n'(i,j) = n(i,j) - \frac{1}{N}\sum_{k=j-(N-1)/2}^{j+(N-1)/2} n(i,k). \tag{5}$$

Since $n(i,j)$ is zero mean, also $n'(i,j)$ is zero mean and (4) is simplified to:

$$\sigma_{n'}^2 = E\left\{n'(i,j)^2\right\} \tag{6}$$

Taking into account (5), the variance of $n'(i,j)$ becomes:

$$\sigma_{n'}^2 = E\left\{\left(n(i,j) - \tfrac{1}{N}\sum_{k=j-\frac{N-1}{2}}^{j+\frac{N-1}{2}} n(i,k)\right)^2\right\},$$

$$\sigma_{n'}^2 = E\left\{\left(\tfrac{N-1}{N}n(i,j) - \tfrac{1}{N}\sum_{\substack{k=j-\frac{N-1}{2}\\ k\neq j}}^{j+\frac{N-1}{2}} n(i,k)\right)^2\right\},$$

$$\sigma_{n'}^2 = \frac{(N-1)^2}{N^2}\sigma_n^2 + \frac{N-1}{N^2}\sigma_n^2 = \frac{N-1}{N}\sigma_n^2. \tag{7}$$

Taking into account that N samples of $n'(i,j)$ are averaged by the filter $F(\bullet)$, the noise variance in $y_2(i,j)$ is given by:

$$\sigma_{n2}^2 = \frac{1}{N}\sigma_{n'}^2 = \frac{N-1}{N^2}\sigma_n^2. \tag{8}$$

Following a similar procedure, the variance of the noise from $y_3(i,j)$ is obtained as:

$$\sigma_{n3}^2 = \frac{N-1}{N}\sigma_{n'}^2 = \frac{(N-1)^2}{N^2}\sigma_n^2. \tag{9}$$

2.2. De-noising the image components

The three image components $y_1(i,j)$, $y_2(i,j)$ and $y_3(i,j)$ are processed separately in order to reduce the noise. There are many possible selections of the de-noising algorithms that can be implemented for this purpose. In our approach we implemented a simple thresholding scheme that shows good filtering results at a relatively low computational cost.

Explicitly, $y_1(i,j)$, $y_2(i,j)$ and $y_3(i,j)$ are processed as:

$$\widehat{y}_t(i,j) = \begin{cases} \frac{\sum_{(l,p)\in\Omega_t} y_t(l,p)}{L^2} & \text{if } m_t(i,j) < \sigma_{n_t} \\ \frac{\sum_{(l,p)\in\Omega_t} W_t(l,p)y_t(l,p)}{\sum_{(l,p)\in\Omega} W_t(l,p)} & \text{otherwise} \end{cases}, t = 1,2,3 \tag{10}$$

where Ω_t is an $L \times L$ search window centered at the current pixel from $y_t(i,j)$ and the weights $W_t(l,p) = 1$ if $y_t(l,p) \in [y_t(i,j) - 2\sigma_{nt}, y_t(i,j) + 2\sigma_{nt}]$ and $W_t(l,p) = 0$ otherwise. The averages $m_t(i,j)$ are computed by the following formula:

$$m_t(i,j) = 1.486MED\{|\Omega_t - MED\{\Omega_t\}|) \tag{11}$$

with MED being the median operator.

The output image is obtained by:

$$\widehat{y}(i,j) = \widehat{y}_1(i,j) + \widehat{y}_2(i,j) + \widehat{y}_3(i,j) \tag{12}$$

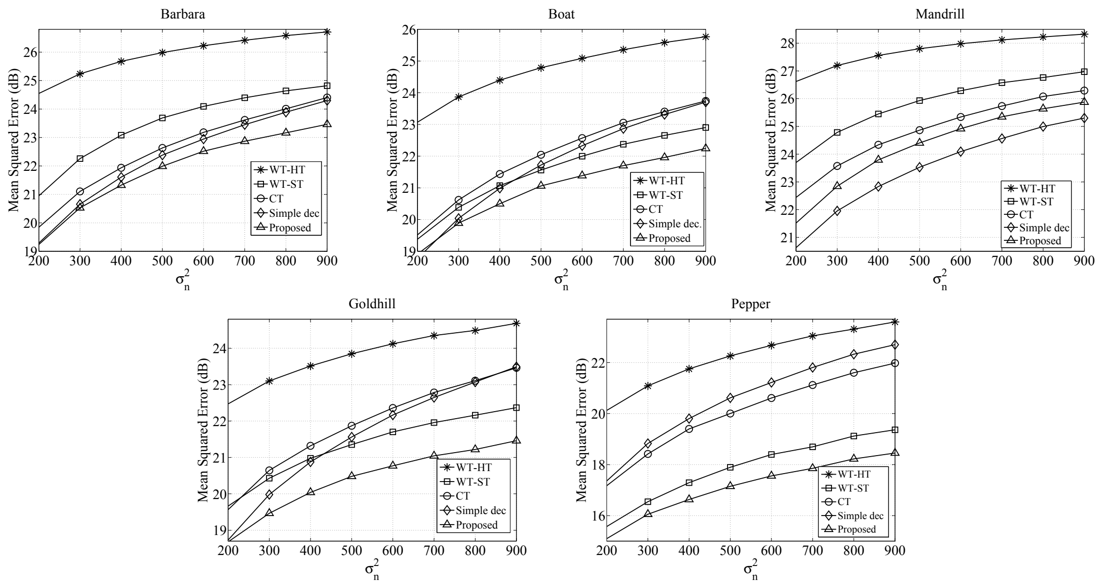

Fig. 2. MSE as function of noise variance: *Barbara* (top left), *Boats* (top middle), *Mandrill* (top right), *Goldhill* (bottom left) and *Pepper* (bottom right).

3. EXPERIMENTS AND RESULTS

In this section we show experimental results comparing the de-noising performances of our proposed algorithm, the wavelet (hard and soft threshold) and contourlet approaches [5, 6, 10] as well as the method in [7]. In our proposed method we have used $N = L = 7$ and for the other algorithms we have followed the guidelines in the corresponding references to select the proper parameters.

To illustrate the performances of the compared algorithms a number of five images are considered (*Barbara*, *boat*, *mandrill*, *goldhill* and *pepper*) with pixel values in the interval $[0, 255]$. The images were corrupted by white Gaussian noise with zero mean and σ_n^2 variance. We have done a large number of experiments for different values of σ_n^2 and the results are plotted in Fig. 2. We can see from this figure that the proposed algorithm has better performances in terms of mean squared error among the compared algorithms for almost all the images. There is only one exception (the *mandrill* image) where the de-noising procedure of [7] performs better than our proposed approach. This is due to the fact that the method in [7] better preserves the very small details such as the mandrill's hair. However, in smother areas of the image, the method proposed by us reduces the noise more effectively as it can be seen also in Fig. 3. One way to improve the preservation of the fine details is to use two different window sizes for the filter $F(\bullet)$ to compute $y_1(i, j)$, $y_2(i, j)$ and $y_3(i, j)$ respectively.

In Fig. 4 we show the de-noising results, of four of the compared algorithms, for the image *peppers*. Also from this figure we can see that our approach provides the best visual impression compared to the other methods.

4. CONCLUSIONS

In this paper, we have introduced a new decomposition scheme for image de-noising. The proposed method shows good de-noising performances in terms of mean squared error and visual impression. Its main advantages are the simplicity of implementation and the possibility to use a large variety of filters into the decomposition process. The preservation of the fine details in the proposed de-noising scheme can be further improved for instance by implementing non-equal window sizes for the two directional filters in Fig. 1 and by using other directional/adaptive filters to perform the image decomposition. These modifications as well as other issues are under consideration and they will be the subject of future publications.

5. REFERENCES

[1] J. Astola and P. Kuosmanen, *Fundamentals of Nonlinear Digital Filtering*, New York: CRC Press, USA, 1997.

[2] A. Foi, R. C. Bilcu, V. Katkovnik, and K. Egiazarian, "Anisotropic Local Approximations for Pointwise Adaptive Signal-Dependent Noise Removal," in *Proceedings of European Signal Processing Conference EUSIPCO 2005*, Antalya, Turkey, Sept 2005.

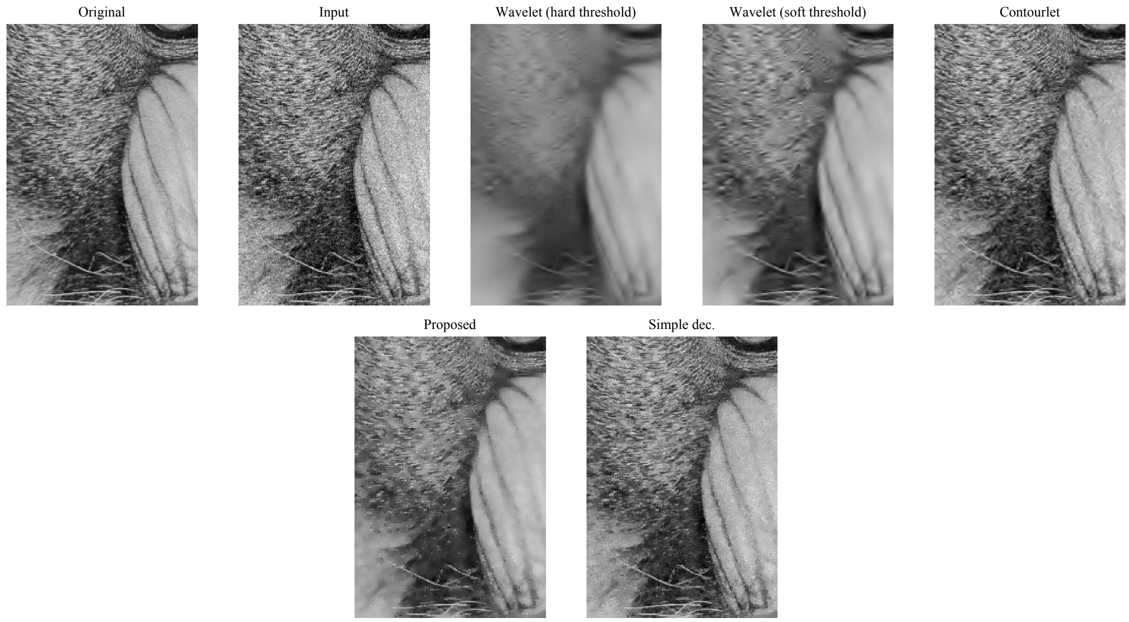

Fig. 3. Results for 'Mandrill' image corrupted with Gaussian noise of $\sigma_n^2 = 400$ (only a part of the image is shown).

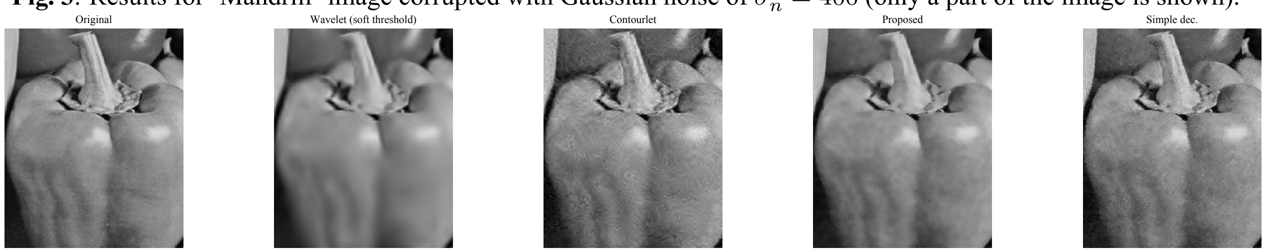

Fig. 4. Results for 'Peppers' image corrupted with Gaussian noise of $\sigma_n^2 = 400$ (only a part of the image is shown).

[3] A. Buades, B. Coll, and J. M. Morel, "Image Denoising by Non-local Averaging," in *Proceedings of IEEE International Conference on Audio Speech and Signal Processing ICASSP 2005*, Philadelphia, USA, March 2005.

[4] J. S. Lee, "Digital Image Smoothing and the Sigma Filter," *in Computer Graphics Image Processing*, vol. 24, pp. 255–269, 1983.

[5] D. L. Donoho and I. M. Johnstone, "Threshold Selection for Wavelet Shrinkage of Noisy Data," in *Proceedings of the 16th IEEE International Conference on Engineering Advances: New Opportunities for Biomedical Engineers*, Baltimore, USA, Nov 1994, pp. A24 – A25.

[6] D. L. Donoho, "De-Noising by Soft-Thresholding," *in IEEE Transactions on Information Theory*, vol. 41, no. 3, pp. 613 – 627, May 1995.

[7] R. C. Bilcu and M. Vehvilainen, "A New Image De-Noising Technique Based on Image Decomposition and Sigma Filtering," *in WSEAS Transactions on Communications*, vol. 4, no. 8, pp. 579–586, Aug 2005.

[8] J. G. Rosiles and M. J. T. Smith, "Image Denoising using Directional Filter Banks," in *Proceedings of IEEE International Conference on Image Processing ICIP 2000*, Vancouver, Canada, Oct 2000, pp. 292–295.

[9] J.-L. Starck, E. J. Candes, and D. L. Donoho, "The Curvelet Transform for Image Denoising," *in IEEE Transactions on Image Processing*, vol. 11, no. 6, pp. 670–684, June 2002.

[10] R. Eslami and H. Radha, "Image Denoising using Translation-Invariant Contourlet Transform," in *Proceedings of the IEEE International Conference on Acoustics, Speech and Signal Processing ICASSP 2005*, March 2005, pp. 557 – 560.

[11] R. C. Bilcu and M. Vehvilainen, "A New Method for Noise Estimation in Images," in *Proceedings of IEEE International Workshop on Nonlinear Signal and Image Processing NSIP 2005*, Saporo, Japan, May 2005.